Original Research Paper

# Preparation of titanium dioxide nanoparticles supported on hexagonal mesoporous silicate (HMS) modified by oak gall tannin and its photocatalytic performance in degradation of azo dye

Ehsan Binaeian [a,*], Nasser Seghatoleslami [a,1], Mohammad Javad Chaichi [b,2], Habib-allah Tayebi [c]

[a] Chemical Engineering Department, Faculty of Engineering, Ferdowsi University of Mashhad, Mashhad, Iran
[b] Faculty of Chemistry, University of Mazandaran, Babolsar, Iran
[c] Textile Engineering Department, Qaemshahr Branch, Islamic Azad University, Qaemshahr, Iran

ABSTRACT

In this study, a new type of photocatalyst, TiO$_2$ based on hexagonal mesoporous silicate (HMS) loaded by different concentrations of natural polyphenol oak gall tannin,OGT, (TiO$_2$–OGT$_x$-HMS, $x$ = 0.3, 0.6, 1 wt.%) was synthesized and used in batch photocatalytic experiments. The synthesized catalysts were characterized using XRD, SEM, EDX and TEM analysis. The analysis showed that tannin was immobilized on the surface of HMS and TiO$_2$ nanoparticles were distributed well and uniform on the surface of OGT-HMS without aggregation, while TiO$_2$ nanoprticles aggregated on the surface of tannin free HMS. The performance of TiO$_2$–OGT$_x$-HMS phtocatalysts for degredation of anionic dye (i.e., Direct yellow 86) in aqueous solution were also compared with the performance of TiO$_2$ (P-25) and TiO$_2$–HMS. TiO$_2$–OGT$_{0.6\%}$-HMS Photocatalyst exhibited higher performance than that of other photocatalysts with the adsorption and degradation efficiencies of 36.7% and 92.2%, respectively. The relative high value of activation energy, 24.8 kJ/mol, confirms the effect of temperature to accelerate the photocatalytic reaction. It was also shown that photocatalytic reaction follows first order kinetic and up to 120 mg/l of dye solution, Langmuir–Hinshelwood (L–H) kinetic model is acceptable.

© 2016 The Society of Powder Technology Japan. Published by Elsevier B.V. and The Society of Powder Technology Japan. All rights reserved.

## 1. Introduction

Toxic wastewater and infected water are the considerable sources of environmental contaminations [1]. Dyes are used in various industries like dyestuffs textile, paper, plastics and pharmaceutical. Recently, reactive dyes have been commonly used because of their advantages such as better dyeing processing conditions and bright colors. Between the reactive dyes, approximately 66% are categorized in azo dyes group which are recognized by nitrogen Π-bound [1]. Direct yellow 86 (i.e., DY86) as an azo dye have been used in different industries such as silk, wool, leather, jute, cotton dying, biological staining, dermatology, veterinary medicine, green ink manufacture, textile dying, and paper printing [2]. DY86 is very venomous and could injure humans or animals eye; so, it should be removed from the environment. Recently, the researches have been focused on the application of hetrogeneous photocatalysts for decomposition of dyes. Especially, this method has a high ability to decompose the organic pollutant. Photocatalysis technique is based on the use of UV-irradiated semiconductors such as TiO$_2$, ZnO, Fe$_2$O$_3$, CdS, ZnS and V$_2$O$_5$. Applications of semiconductors as the photocatalysts have been reported in the literature because of their environmental-friendly advantages in the saving of resources such as water, energy, chemicals, and other cleaning materials [3]. Photocatalysts are used either in suspension form or in immobilized form on a support during photocatalitic processes. Kansal et al. compared the performance of suspension of TiO$_2$, ZnO, CdS and ZnS in the presence of UV radiation for degradation of biebrich scarlet (BS) dye. Performance of ZnO in degradation of dye was better than the other catalysts [4].

The photocatalytic activity of TiO$_2$ suspension catalyst at different sizes for degradation of Congo red was also studied by Farbod and Khademalrasool [5]. In practice, immobilization of photocatalyst on a support is preferred, because it does not need

* Corresponding author. Tel.: +98 11 33209948.
E-mail addresses: e.binaeian@qaemshahriau.ac.ir (E. Binaeian), slami@um.ac.ir (N. Seghatoleslami), jchaichi@yahoo.com (M.J. Chaichi), Tayebi_h@yahoo.com (H.-a. Tayebi).
[1] Tel.: +98 51 38805033.
[2] Tel.: +98 11 35302386.

the separation of downstreams such as separation of fluid-particle or recycling of photocatalyst. So, many researches have been focused on immobilization of photocatalyst on different supports. Immobilization of $TiO_2$ on the silicate support such as MCM-41 [6], gold nanoparticles loaded amino and mercapto functionalized TiMCM-41 [7], $TiO_2$ loaded SBA-15 [8], immobilized $TiO_2$ on Na-HZSM-5 as a composite [9], in situ synthesize of NaA and CaA zeolite-supported titania [10], immobilized nickel on p-zeolite [11], tin and titanium incorporated rice husk silica nanocomposite [12] are some researches which have been investigated for immobilization of photocatalysts on different supports. Photocatalysts such as $TiO_2$ may not be distributed well on the surface of supports due to high energy and the desire for aggregation; therefore, it leads to aggregation of the particles. So, to overcome this trouble, inorganic supports like silicates can be functionalized by organic polymers. These functional groups can coordinate with photocatalysts by their ligands. Thus, well distribution of metalic catalysts occurs on the surface of support. Hence, catalytic activity of supported catalysts is retained [13]. Tannins which are extremely available in plants, are the water-soluble multi phenolic hydroxyls. Tannins are able to chelate with many types of metal ions by their condensed phenolic hydroxyls [13]. This characteristic of tannins shows that they can act as a suitable agent to immobilize metals. Huang et al. showed that tannin can form covalent bonds with amine groups of aminated mesoporous silica through crosslinking of aldehyde [14]. Binaeian et al. [15] investigated about the effect of tannin immobilization on the surface of mesopooeous silicate (HMS) for the removal of direct yellow 86 dye. They showed that tannin could enhance the ability of HMS for dye removal from aqueous solution. In the present study, $TiO_2$ supported on oak gall tannin-immobilized hexagonal mesoporous silicate ($TiO_2$–OGT-HMS) were synthesized as a new photocatalyst. These photocatalysts were characterized by XRD, SEM, EDX and TEM analysis. Photocatalytic activity of $TiO_2$–OGT-HMS for degradation of direct yellow 86 (i.e., DY86) was examined under UV light irradiation. The effect of some parameters such as pH of solution, photocatalyst dosage, temperature and dye concentration on degradation of dye solution were studied. To fit the experimental data, Langmuir–Hinshelwood (L–H) kinetic model was applied.

## 2. Materials and methods

### 2.1. Materials

$TiO_2$ nanocatalyst ($TiO_2$, P-25, anatase 80%–rutile 20%, 51 $m^2$/g, 20 nm) was purchased from Degussa. The UV light source was a 8 W low-pressure mercury lamp with maximum output under 400 nm that was bought from Philips, Holland. Titanium isopropoxide (TIP) with 99.99% purity was purchased from Sigma–Aldrich. Tetraethyl ortho silicate (TEOS, $SiC_8H_{20}O_4$), ethanol ($C_2H_5OH$), methanol ($C_2H_3OH$), hydrochloric acid (HCl), dodecylamine ($C_{12}H_{25}NH_2$), glutaraldehyde, 3-Aminopropyltriethoxysilane (APTES), sodium carbonate ($Na_2CO_3$), $H_2SO_4$ and NaOH for the adjustment of pH, $Na_2HPO_4$ and $NaH_2PO_4$ for the preparation of buffer solution and deionized water were purchased from Merck. Furthermore, anionic dye (i.e., Direct yellow 86 or DY86 with $\lambda_{max}$ = 384 nm) was obtained from Dystar, Germany. Extraction of tannin from oak gall powder was carried out in the presence of water and methanol mixture as a solvent with a ratio of 1:1. Finally, the solvent was evaporated at 333 K and a pressure of 10 mmHg [16].

### 2.2. Preparation of tannin-HMS particles

After synthesize of HMS using the method explained by Pinnavaia [17], 1 g of HMS and 10 mL of APTES were stirred with 50 mL of normal hexane. It was carried out under the reflux for

6 h. Then, after filtration, the prepared sample washed with acetone and deionized water consecutively and dried for 24 h under vacuum at 323 K (Aminated HMS) [18]. Phenolic rings in the tannin structure have a nucleophilic tendency, so glutaraldehyde as a electrophilic agent could creat covalent bond with the rings. Glutaraldehyde could also react with the amino group of aminated-HMS. Hence, tannin could be immobilized on the surface of aminated-HMS with the presence of glutaraldehyde as the cross-linking agent to form covalent bond [19]. Previously, we prepared OGT-HMS nanoparticles with different concentrations of oak gall tannin solutions [15]. Briefly, aminated HMS (A-HMS) was mixed with 0.3, 0.6 and 1 wt. % oak gall tannin solutions. After stirring of mixtures for 2 h, glutaraldehyde (50%, w/w) was added. Then, the mixtures were stirred for one day at room temperature. Subsequently, the brown tannin-HMS nanopowder ($OGT_x$-HMS) was obtained after filtering, washing with deionized water and drying in a vacuum oven at 323 K.

### 2.3. Preparation of $TiO_2$–OGT-HMS and $TiO_2$–HMS

To prepare $TiO_2$–HMS photocatalyst, 0.5 g of HMS and 50 mL of ethanol were mixed. Then 0.1 M nitric acid was added. After that, 1.8 g of titanium isopropoxide as precursor of $TiO_2$ was mixed with suspension. The prepared suspension was heated at 323 K and mixed for 5 h. Next, the prepared suspension was filtrated and dried at 373 K for 6 h in a vacuum oven. The dried sediment was calcinated in a furnace at 673 K for about 4 h. Then, about 0.5 g of each types of OGT-HMS were processed by titanium isopropoxide according to the described procedure. Finally, $TiO_2$–$OGT_x$-HMS photoctalysts were prepared.

### 2.4. Characterization

X-ray diffraction (XRD) patterns of samples were carried out using refractometer (35 kV, 28.5 mA and 298 K, Philips instruments, Australia) where copper anode was used as a radioactive source. The concentration of tannin in solutions was measured using ultraviolet–visible spectrophotometer (6310, JENWAY, UK). Dye solutions were also analyzed by spectrophotometer prior and after phtocatalysis process. Transmission electron microscopy (TEM) images of the photocatalysts were prepared (TEM, CM120, PHILIPS, Holland, 150 kV). Sample surface morphologies were analyzed by a HITACHI S-4160 scanning electron microscopy (SEM) equipped with an energy dispersive X-ray spectroscopy (EDAX).

### 2.5. Photo-degradation experiments

Experimens were carried out in a dark and closed box which UV radiation source is 8 W low-pressure mercury lamp with a wavelength of 400 nm. 50 mL of DY86 solutions (40, 60, 80, 100 and 120 ppm) and different amounts of photocatalyst (0.025, 0.05, 0.075, 0.1, 0.15, 0.2 and 0.3 g) were magnetically stirred in 100 mL beaker. Then, photocatalytic performance of $TiO_2$–$OGT_x$-HMS ($x$ = 0.3%, 0.6% and 1%), $TiO_2$–HMS and $TiO_2$ (P-25) were compared. Before turning on of the UV lamp, photocatalysts were stirred in a dark position for 60 min to achieve adsorption equilibrium. Then, UV lamp was turned on and the initial dye concentration ($C_0$) was measured at the optimum pH. $C_0$ was also considered as the initial dye concentration after dark adsorption. The samples were withdrawn regularly (0, 15, 30, 60, 90, 120, 150, 180, 210 and 240 min) from the beakers and the concentrations of DY86 in equilibrium state ($C_e$) were obtained. The effects of pH (3–10) and temperature (298, 303, 308 and 313 K) on the photocatalytic activities of photocatalysts were also evaluated. Photocatalytic degradation of DY86 was expressed as fallowing relation:

Photocatalytic degradation $\% = [(C_0 - C_e)/C_0] \times 100$     (1)

# 3. Results and discussion

## 3.1. Immobilization of tannin on HMS

Oak gall tannin is categorized in hydrolysable tannin group. As can be seen in Fig. 1, there are galloyles in the structure of hydrolysable tannin containing adjacent hydroxyl groups which have strong affinity to metal ions. Also, carbon atoms of phenolic rings have nucleophilic tendency and tannin could form covalet bonds with amino groups loaded on the surface of HMS particles and in the presence of glutaraldehyde which acts as a cross-linking agent [13]. The results reveal that the loading of HMS by 0.3%, 0.6% and 1% tannin solutions was 29%, 34% and 39%, respectively. These results were read from calibration curve of tannin solution in the range of 5–30 ppm.

## 3.2. Proposed mechanism for synthesize of TiO$_2$–OGT–HMS

Fig. 2 shows the recommended mechanism for preparation of TiO$_2$–OGT-HMS photocatalyst. Since the standard potential of titanium in the standard electrode table is negative, so the tendency for absorption of oxygen is so high. The oak gall tannin has phenolic rings with adjacent OH which have high absorption tendency and chelating ability. Due to the high oxygen affinity of titanium, it supplies required oxygen from solution and adjacent hydroxyl of phenols. Therefore, titanium intracts with oxygen and makes five member chelates with adjacent phenolic hydroxyls which are stable thermodynamically. According to the Fajanz method [20], silver and chloride ions in AgCl solution are adsorbed on silver chloride deposite. So, TiO$_2$ could be adsorbed on tannin due to the oxygen tendency of TiO$_2$. After that, uniform distribution of TiO$_2$ will occur on the surface of HMS nanoparticles. After preparation of TiO$_2$–OGT-HMS and For phase transformation of TiO$_2$ from amorph to anatase, calcination was performed at 400 °C for about 4 h.

## 3.3. Characterization of synthesized photocatalysts

The FTIR spectra of HMS and OGT-HMS in the range of 400–4000 cm$^{-1}$ have been reported in our recent published paper and the loading of HMS by tannin have been proved [15].

Fig. 3 shows the SEM images of HMS and OGT$_{0.6\%}$-HMS nanoparticles. As seen in Fig. 3(a), HMS nanoparticles are spherical and uniform. Fig. 3(b) shows colonies of OGT-HMS particles. It can be seen that the particle size increased due to the coverage of HMS surface by tannin. So, this image shows that tannin is well established on the support.

EDX spectra of TiO$_2$–HMS and TiO$_2$–OGT$_x$-HMS photocatalysts are shown in Fig. 4. The EDX analysis of TiO$_2$–HMS (Fig. 4(a)) shows the presence of Ti, O and Si. The EDX spectra of the composite TiO$_2$–OGT$_x$-HMS also confirm the presence of O, Ti, Si and C. As can be seen in Fig. 4(c), EDX spectrum of TiO$_2$–OGT$_{0.6\%}$-HMS shows higher peak for Ti in comparison with two other types (Fig. 4(b and d)) and this is because of well distribution of TiO$_2$ on the surface of OGT-HMS. EDX sepectrum of TiO$_2$–OGT$_{1\%}$-HMS composite exhibits higher peak for C in comparison with TiO$_2$–OGT$_{0.3\%}$-HMS, TiO$_2$–OGT$_{0.6\%}$-HMS. More amounts of tannin leads to more presence of phenolic groups in the catalyst structure and thus increases the amounts of carbons. The important point is that the Ti peak for three groups of photocatalysts containing tannin is higher than that of without tannin. Phenolic groups of tannin are connected to the aminated Si–O–Si groups of HMS. But, There are no phenolic groups in the HMS structure; therefore, more suitable distribution of TiO$_2$ on the surface of HMS containing tannin leads to increase of degradation efficiency of DY86 [21].
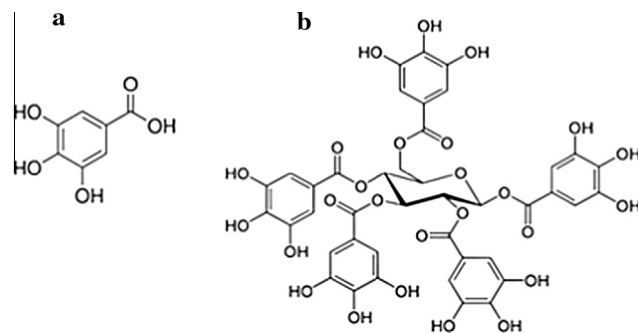


**Fig. 1.** The structure of acid gallic (a) and pentagallyolglucose (b).

Fig. 5 shows the XRD pattern of the TiO$_2$–OGT$_{0.6\%}$-HMS after calcination at 673 K. All peaks are compatible with the range of standard spectrum (JCPDS No. 84-1286). XRD analysis of the sample exhibits sharp peaks at $2\theta = 25°$ and $2\theta = 48°$, indicating the presence of anatase phase in the TiO$_2$ structure. Diffraction patterns and planes of anatase phase of TiO$_2$ structure obviously agree with the study of Cetinkaya et al. [21].

Transmission electron microscopy (TEM) images of the TiO$_2$–HMS and TiO$_2$–OGT$_x$-HMS are shown in Fig. 6. As can be seen in Fig. 6(a), TiO$_2$ particles aggregate on the surface of HMS. In the absence of tannin, there is no proper ability for immobilization of Ti on the surface of HMS. Due to the high surface energy of Ti particles, they have a great tendency for aggregation during each process. As Fig. 6(b–d) demonstrate, Ti particles do not aggregate on the surface of OGT$_x$-HMS in comparison with HMS, this is because of high adsorption of Ti on the phenolic groups of tannin, preferably adjacent phenolic groups for changing into TiO$_2$. So, with formation of five member chelate, TiO$_2$ was well distributed on the surface of HMS [13,14]. As can be seen in the TEM images of TiO$_2$–OGT$_x$-HMS, loading of HMS by the least concentration of tannin (0.3% tannin solution) can also prevent the aggregation of TiO$_2$ on the surface in comparison with tannin free HMS. So, it indicates the effective chelating property of tannin.

## 3.4. Effect of pH

The Effect of pH on photocatalytic degradation of DY86 in the range of 3–11, an initial dye concentration of 40 ppm, 0.1 g of the various photocatalysts and contact time of 150 min were studied. The adjustment of pH was carried out using 1 M of HCl or NaOH. After achieving the equilibrium adsorption in dark condition, dye solutions were put in the exposure of UV irradiation for 150 min. The photocatalytic performance of different photocatalysts for degradation of DY86 is shown in Fig. 7.

As seen in Fig. 7, at lower pH, degradation efficiency for all catalysts increases. Lower pH produces hydroxyl radicals and increases the surface area. Meanwhile, OH groups of tannins take protons at lower pH and whereas DY86 is an anionic dye, dye adsorption on the surface of photocatalyst increases [22].

On the other hand, at pH about 3 that is less than pH$_{pzc}$ of TiO$_2$, the TiOH$_2^+$ groups which are dominant groups are produced and the electrostatic attraction force causes the adsorption of anionic dye molecules on the surface of the photocatalyst [1,23].

These two phenomena are synergistic and could enhance the adsorption of DY86 on the photocatalyst surface and improve the efficiency of photocatalytic degradation. So, the pH of 3 was considered as the optimum value. Also, it should be considered that the generation of hydroxyl radicals in the acid solution and in the presence of oxygen improves the decomposition and degradation of dye.
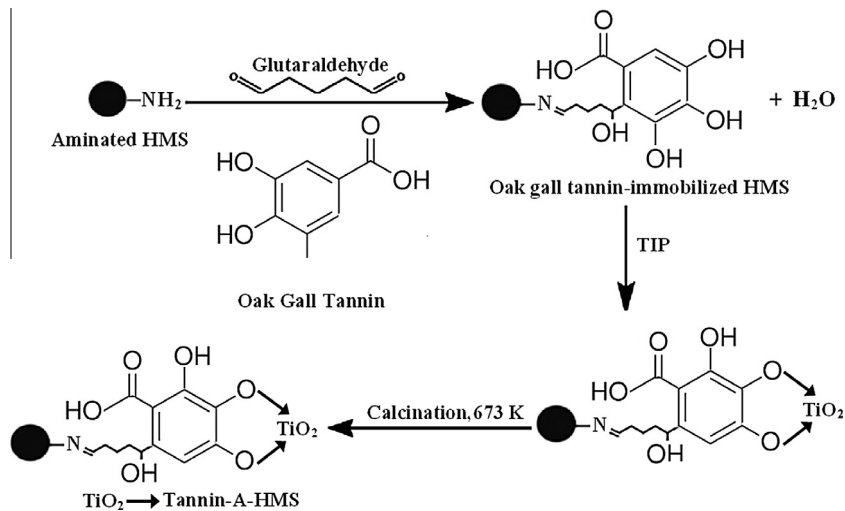
**Fig. 2.** Proposed mechanism for synthesize of $TiO_2$–OGT-HMS photocatalyst.
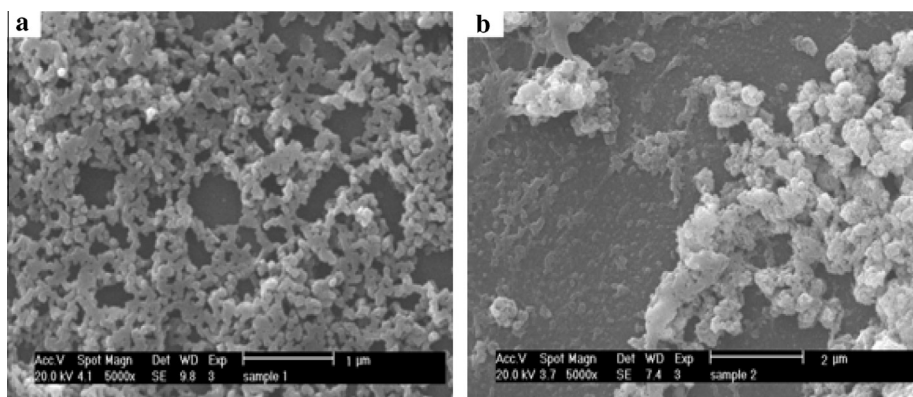


**Fig. 3.** SEM images of HMS (a) and $OGT_{0.6\%}$-HMS (b).

## 3.5. Comparison of photocatalysts performance

Performance of various catalysts for the removal and degradation of DY86 before and after UV radiation is shown in Fig. 8. Without the catalyst, almost no change was observed in dye concentration. Potential of the valence band ($h_{VB}^+$) is positive enough to produce hydroxyl radicals in the surface of semiconductor and the conduction band ($e_{CB}^-$) is sufficiently negative to reduce oxygen molecules in the solution. Generated hydroxyl radicals are the strong oxidizing agents; so, they can oxidize dyes or organic contamination on the surface and surface close of $TiO_2$ (0–500 mμ). With increase of distance from the surface, the rate of hydroxyl radicals reaction with organic pollutions or dyes increases [24]. Dye adsorption on the surface of photocatalysts was measured before the beginning of the reaction for 1 h (without UV). Photocatalysts containing tannin exhibited higher adsorption efficiency in comparison with $TiO_2$–HMS and $TiO_2$. It shows the effect of tannin as a functional group for adsorption of dye (see Table 1).

As can be seen in Fig. 8, $TiO_2$–$OGT_{0.6\%}$-HMS shows higher photocatalytic activity than that of $TiO_2$–$OGT_{0.3\%}$-HMS, $TiO_2$–$OGT_{1\%}$-HMS, $TiO_2$–HMS and P-25. All three photocatalysts containing tannin exhibited higher performance than that of $TiO_2$–HMS and P-25. With increase of oak gall tannin concentration from 0.3% to 0.6%, loading of tannin on the surface of HMS increased. So, photocatalytic degradation of DY86 increased up to 92.22%. It is observed with increase of tannin solution concentration from 0.6% up to 1%, in spite of the increase in the loading of tannins on the support, photocatalytic degradation decreases. Additional content of tannin loaded on the surface of HMS limits the access of dye molecules to the surface of $TiO_2$ nanoparticles. So, $TiO_2$–$OGT_{0.6\%}$-HMS showed the highest photocatalytic activity [13].

Performance of $TiO_2$–HMS in photocatalytic degradation of DY86 is higher than P-25 because of uniform distribution and less aggregation of $TiO_2$ on the support. As can be seen in Fig. 8, Photocatalytic degradation of dye depends on the adsorption of dye on the surface of photocatalyst. With the increase of dye adsorption before the beginning of the photocatalytic reaction, the rate of photocatalytic degradation reaction increases. This fact is compatible with the theory of heterogeneous catalyst (L–H Model) [25]. Since the photocatalytic performance of $TiO_2$–$OGT_{0.6\%}$-HMS was higher than the other photocatalysts, it was used in the subsequent experiments.

## 3.6. The effect of photocatalyst dosage

One of the most important parameters affecting the efficiency of photocatalytic degradation process is the concentration or dosage of the photocatalyst. To determine the optimum dosage of $TiO_2$–$OGT_{0.6\%}$-HMS, degradation of DY86 at various dosage of 0–0.3 g was examined. As can be seen in Fig. 9, increase of the photocatalyst dosage up to 0.1 g, improves the efficiency of photocatalytic degradation of DY86. With the increase of the photocatalyst dosage more than the optimum value, no significant effect was
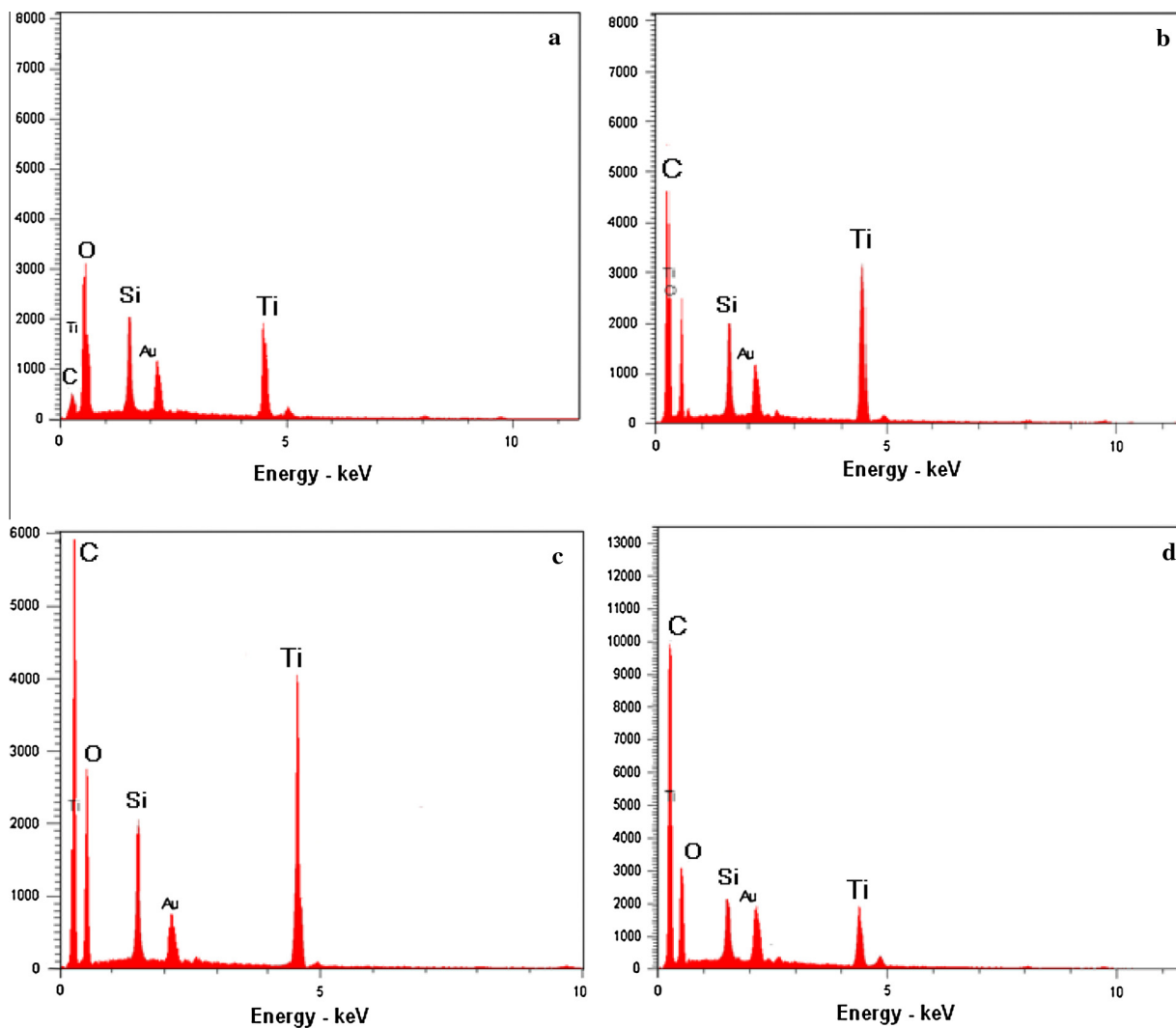
**Fig. 4.** EDX spectra of TiO$_2$–HMS (a), TiO$_2$–OGT$_{0.3\%}$-HMS (b), TiO$_2$–OGT$_{0.6\%}$-HMS (c), and TiO$_2$–OGT$_{1\%}$-HMS (d).
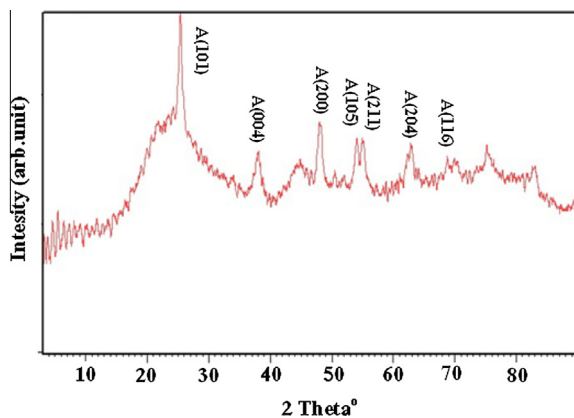


**Fig. 5.** XRD pattern of TiO$_2$–OGT$_{0.6\%}$-HMS.

observed for the efficiency of the process. This is because of lower diffusion of UV radiation into dye solution and lack of access to the surface of photocatalyst. So, 0.1 g of TiO$_2$–OGT$_{0.6\%}$-HMS photocatalyst was considered as the optimum dosage and subsequent tests were carried out with this dosage.

### 3.7. Kinetic of process

In the most researches that have been studied about photocatalytic degradation of organic components, first order model was considered as a kinetic of reaction according to the following relation:

$$r_i = -dC_i/dt = k_{obs}C_i \tag{2}$$

where $r_i$ (mg/l.min) is the rate of dye degradation, $t$ (min) is UV radiation time, $C_i$ (mg/l) is dye concentration and $k_{obs}$ (1/min) is the observed rate constant (experimental) of first order reaction. With the integration of Eq. (2), we have:

$$\ln(C/C_0) = -k_{obs}t \tag{3}$$

where $C_0$ (mg/l) is the initial dye concentration. $k_{obs}$ depends on the initial dye concentration ($C_0$). The controlling step of the photocatalytic reaction in the presence of TiO$_2$ is the adsorption of reactant on the surface of photocatalyst [25].

The Langmuir–Hinshelwood (L–H) model is one of the most common kinetic models which is used for the expression of kinetics of heterogeneous catalytic reactions. Data obtained from photocatalytic degradation of DY86 were fit with Langmuir–Hinshelwood (L–H) kinetics model. In this model, it is assumed
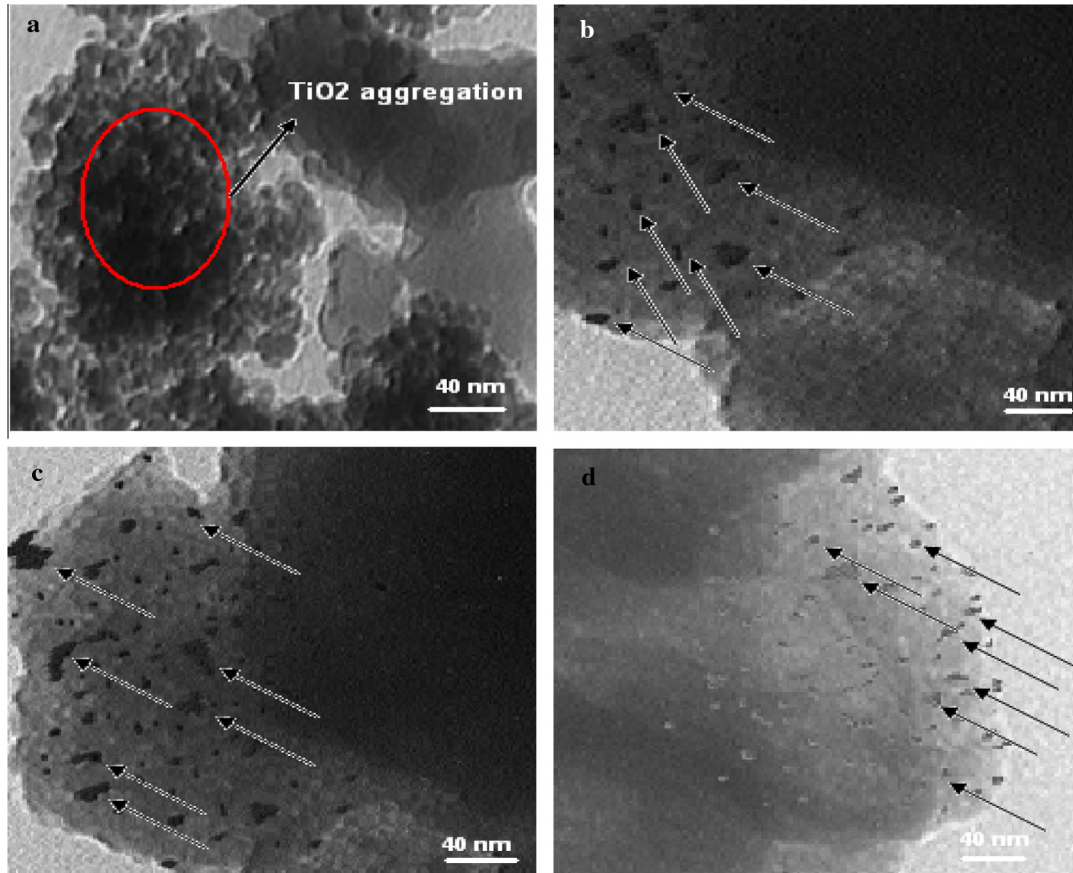
**Fig. 6.** TEM images of TiO$_2$–HMS (a), TiO$_2$–OGT$_{0.3\%}$-HMS (b), TiO$_2$–OGT$_{0.6\%}$-HMS (c) and TiO$_2$–OGT$_{1\%}$-HMS (d).
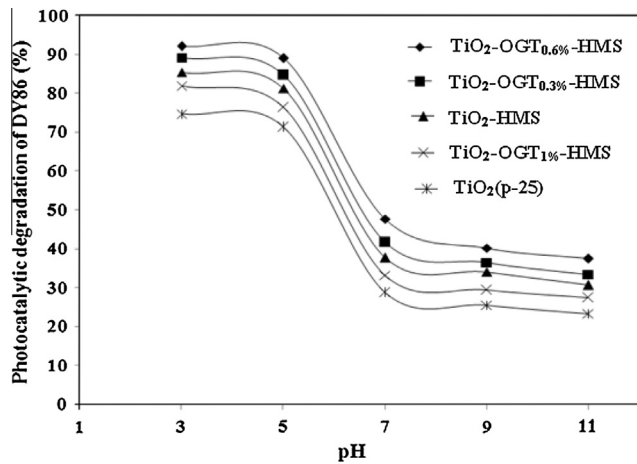


**Fig. 7.** Effect of pH on degradation of DY86 in the presence of different photocatalysts ($C_0$ = 40 mg/l, 0.1 g of the photocatalysts, contact time of 150 min).
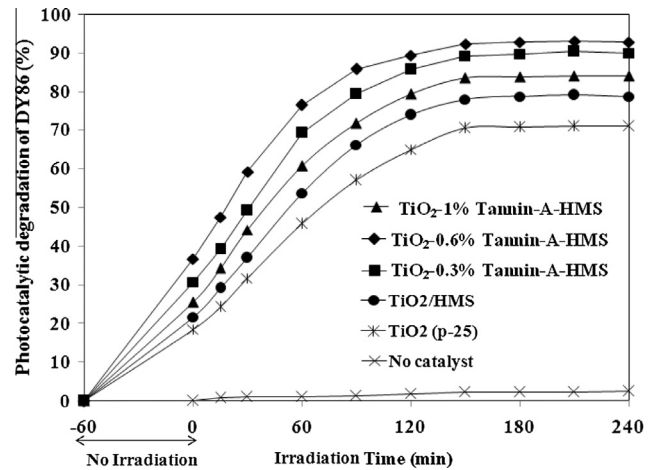


**Fig. 8.** Comparison of different photocatalysts performance in the presence and absence of UV radiation (0.1 g of photocatalysts, pH = 3, $C_0$ = 40 mg/l).

that the adsorption of dye occurs on the photocatalyst surface before the photocatalytic reaction. L–H model is defined as follows:

$$r = -dC/dt = k_rKC/(1 + KC) \qquad (4)$$

where $r$ (mg/l min) is the rate of dye degradation which it changes with time. In this equation, $r_0$ is defined as a function of initial dye concentration, $C_0$, or as a function of the equilibrium concentration of dye, $C_0$, and can be achieved after adsorption process (absence of UV radiation). For a system consists of one reactant, a linear relationship is obtained as follows [25]:

$$1/k_{obs} = C_0/k_r + 1/(k_rK) \qquad (5)$$

If a reaction follows the L–H model, $1/k_{obs}$ will be proportional with $C_0$. So, if $KC \ll 1$, the L–H model changes into the first-order kinetic model:

$$-\ln(C/C_0) = k_{obs}t \qquad (6)$$

The results were listed in Table 1. According to the diagrams of Fig. 10 and $R^2$ values of Table 1, it is observed that the decrease in dye concentration during exposure time follows the pseudo-first-order kinetic model. In the subsequent experiments, the same method was used to determine $k_{obs}$.

**Table 1**
Comparison of different photocatalysts performance for adsorption and degradation of DY86 ($C_0$ = 40 mg/l, pH = 3, 0.1 g of photocatalysts).

| $R^2$ | Degradation (%) | $k_{obs}$ (min$^{-1}$)[b] | Efficieny of adsorption (%)[a] | Photocatalyst |
|-------|-----------------|--------------------------|--------------------------------|----------------|
| 0.987 | 92.2 | 0.014 | 36.7 | TiO$_2$–OGT$_{0.6\%}$-HMS |
| 0.994 | 89.2 | 0.012 | 30.7 | TiO$_2$–OGT$_{0.3\%}$-HMS |
| 0.996 | 83.5 | 0.010 | 25.5 | TiO$_2$–OGT$_{1\%}$-HMS |
| 0.993 | 78.0 | 0.009 | 20.0 | TiO$_2$-HMS |
| 0.997 | 70.5 | 0.007 | 16.0 | TiO$_2$ (P-25) |

[a] The values of adsorption efficiency is calculated during first 60 min without UV radiation.
[b] The values of $k_{obs}$ is calculated since the beginning of UV irradiation up to equilibrium condition (150 min).
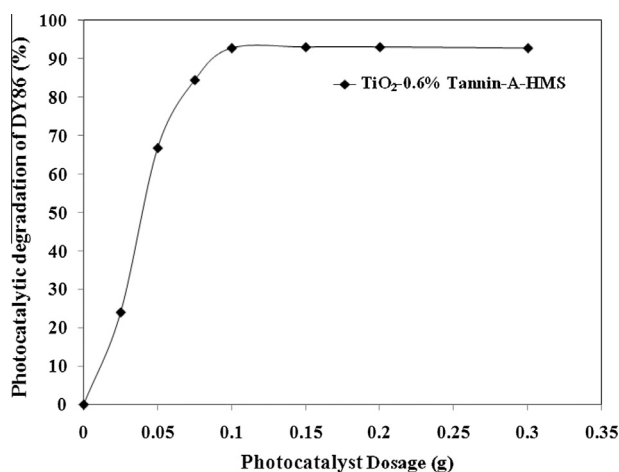


**Fig. 9.** The effect of photocatalyst dosage on photocatalytic degradation of DY86 ($C_0$ = 40 mg/l, pH = 3, contact time of 150 min).



**Fig. 10.** Compatibility of experimental data with the first order reaction model for calculation of $k_{obs}$ in the presence of different photocatalysts ($C_0$ = 40 mg/l, pH = 3 and 0.1 g of catalysts).
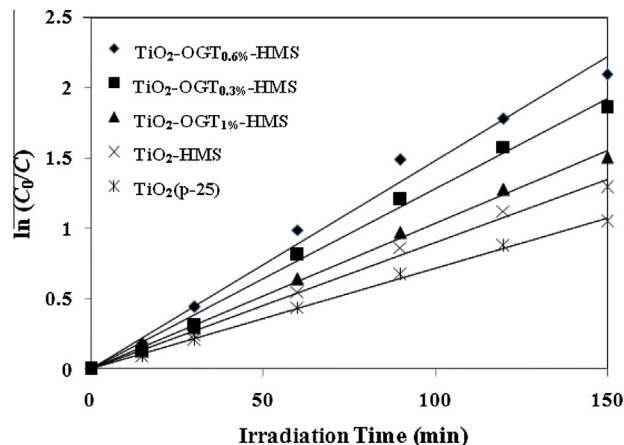
### 3.8. The effect of initial dye concentration on $k_{obs.}$ and degradation of DY86

The adsorption and photocatalytic degradation of dye in different concentrations and in the presence of UV were tested. As can be seen in Fig. 11, the increase of initial concentration causes the lower efficiency of photocatalytic degradation (Fig. 11).

The experimental results in form of reverse values of $k_{obs}$ versus $C_0$ for TiO$_2$–OGT$_{0.6\%}$-HMS are plotted and shown in Fig. 12 and Table 2. High values of $R^2$ in the large ranges of concentrations confirm that the kinetic of photocatalytic degradation follows the L–H model. Also, as can be seen in Fig. 12, the kinetics of degradation follows the L–H model up to 120 mg/l and with further increase in dye concentration, $k_{obs}$ values are much less than that of calculated from L–H model. In fact, with the increase of concentration, the intensity of UV radiation that reaches to the surface of TiO$_2$ particles is reduced and part of the radiation is absorbed by DY86.
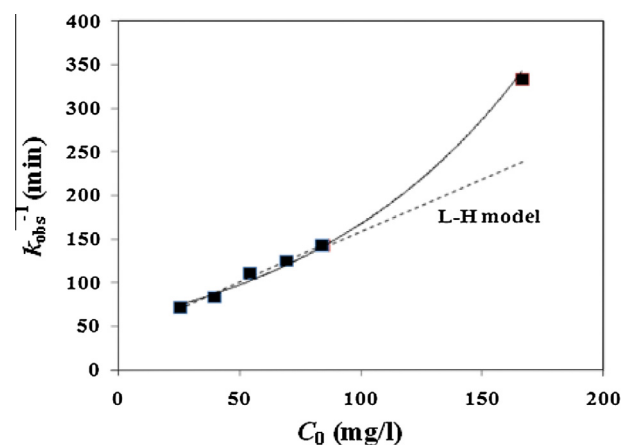
### 3.9. Effect of temperature

As can be seen in Fig. 13, with the increase of temperature from 298 up to 313 K, degradation of DY86 increases. Increase the temperature, causes the increase of free radicals reactivity (OH·), which is very helpful and effective for degradation of organic pollutants [26]. The increase of temperature prevents the recombination of valence band holes ($h_{vb}^+$) and conduction band electrons ($e_{CB}^-$). Also, the increase of temperature, increases the rate of dye oxidation on the solid–liquid interface. On the other hand, rising temperature decreases the solubility of oxygen in water which is not desirable.
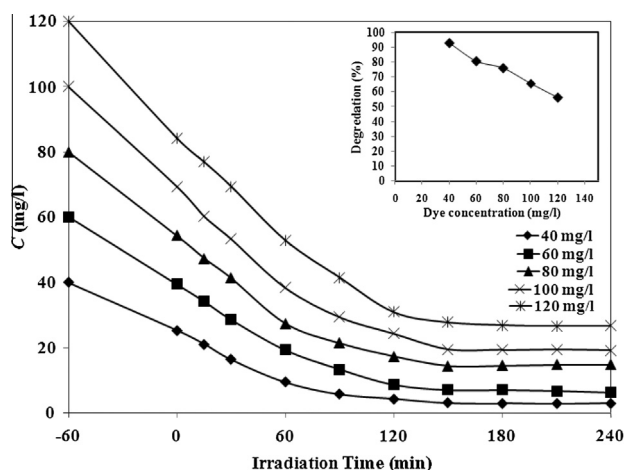


**Fig. 11.** The effect of initial dye concentration on the photovatalytic degradation of DY86 (pH = 3 and 0.1 g of TiO$_2$–OGT$_{0.6\%}$-HMS).



**Fig. 12.** The effect of initial dye concentration on the rate constant of photocatalytic degradation ($k_{obs}$) (dash line is corresponded to the L–H model, pH = 3, 0.1 g of TiO$_2$–OGT$_{0.6\%}$-HMS).

The temperature higher than 318 K causes evaporation of the solution during the experiments. So, the reaction was not carried out at above 313 K [25].

**Table 2**
Kinetic data of photocatalytic degradation of DY86 by $TiO_2-OGT_{0.6\%}$-HMS (pH = 3 and 0.1 g of photocatalyst).

| $R^2$ | $K$ (l/mg) | $k_r$ (mg/l min) | $1/k_{obs} = C_0/k_r + 1/(k_r K)$ | Initial dye concentration (mg/l) at the beginning of radiation UV | Initial dye concentration (mg/l) befor UV radiation (mg/l) |
|---|---|---|---|---|---|
| 0.986 | 0.032 | 0.800 | $k_{obs}^{-1} = 1.25C_0 + 38.56$[a] | 25.3 | 40.0 |
| | | | | 39.5 | 60.0 |
| | | | | 54.3 | 80.0 |
| | | | | 69.3 | 100.0 |
| | | | | 84.2 | 120.0 |

[a] This equation was considered during photocatalytic reaction (150 min) and up to 150 mg/l.
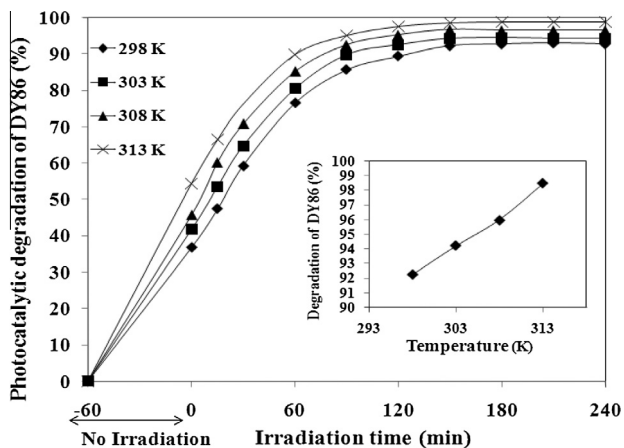


**Fig. 13.** The effect of temperature on the photocatalytic degradation of DY86 (0.1 g of $TiO_2-OGT_{0.6\%}$-HMS, pH = 3, $C_0$ = 40 mg/l, 240 min irradiation time).

Effect of temperature on the reaction rate constant was investigated by plotting $\ln(C_0/C)$ versus the radiation time in the range of 298–313 K (Fig. 14). For all of the rate constants, the favorite $R^2$ values were obtained which are showing the photocatalytic degradation of DY86 follows the first-order kinetic.

The calculated reaction rate constants in the range of 298–313 K are shown in Table 3. As can be seen, with the increase of temperature, the reaction rate constant increases. Generally, the rising temperature improves the reaction rate constant. This matter was also observed and confirmed by Wu and coworkers [27]. They studied about degradation of RR2 dye in the presence of $TiO_2$ and UV using US (ultrasonic) technology. Qi et al. also showed that increase of the temperature from 307 up to 373 K in the pres-
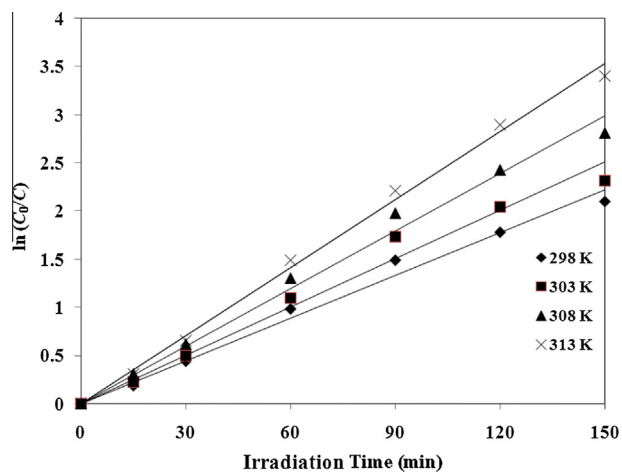


**Fig. 14.** The effect of temperature on the reaction rate constant at different temperature (0.1 g of $TiO_2-OGT_{0.6\%}$-HMS, pH = 3, $C_0$ = 40 mg/l, 150 min irradiation time).

**Table 3**
Rate constants of first order photocatalytic reaction at different temperature (0.1 g of $TiO_2-OGT_{0.6\%}$-HMS, pH = 3, $C_0$ = 40 mg/l, irradiation time of 150 min).

| $\Delta S$ (J/mol K) | $\Delta H$ (kJ/mol) | $E_{activation}$ (kJ/mol) | $R^2$ | $k$ (min$^{-1}$) | Temperature (K) |
|---|---|---|---|---|---|
| −206 | 22.3 | 24.8 | 0.987 | 0.014 | 298 |
| | | | 0.971 | 0.017 | 303 |
| | | | 0.988 | 0.019 | 308 |
| | | | 0.996 | 0.023 | 313 |

ence of titanium nanoparticles and UV radiation, increase the reaction rate constant and therefore increase the rate of photocatalytic degradation of Methyl Orange [28]. In our research, the value of activation energy of the reaction was calculated 24.8 kJ/mol using Arrhenious equation. Qi et al. [28] also reported that the activation energy for photocatalytic degradation of Methyl Orange is 27.7 kJ/mol. Wu and Yu [27] reported that the activation energy for degradation of reactive red 2 at three different pH of 4, 7 and 10 are 6.6, 11.6 and 21.3 kJ/mol, respectively. The relative high value of activation energy confirms the effect of temperature to accelerate the photocatalytic degradation of DY86 in the presence of $TiO_2$. The enthalpy and entropy were calculated using the Eyring equation [27,28], whose values are 22.3 kJ/mol and −205.6 J/mol K, respectively. Large and negative value of entropy is compatible with the interaction between molecules of adsorbed DY86 and surface oxidizing agent that is produced by irradiation of UV on the surface of $TiO_2$.

## 4. Conclusion

In this research, it was shown that $TiO_2$ particles could be well distributed on the surface of HMS loaded by three different concentrations of oak gall tannin solutions. High chelating ability of adjacent OH in phenolic rings of tannin and high oxygen affinity of titanium cause the intraction of titanium with oxygen of phenolic rings which is stable thermodynamically. Increase of particle size and coloni formation are representative of surface coverage of HMS by tannin. These photocatalysts exhibited higher performance than that of common $TiO_2$–HMS and $TiO_2$ (P-25). The results demonstrated that $TiO_2$ supported on HMS loaded by 0.6% oak gall tannin solution ($TiO_2-OGT_{0.6\%}$-HMS) has the highest performance between the other photocatalysts. It was also found that the photocatalytic degradation of DY86 increases with the increase of dye adsorption (without UV radiation) on the surface of photocatalyst. So, $TiO_2$–OGT-HMS photocatalysts showed higher adsorption efficiency than that of $TiO_2$–HMS and $TiO_2$. This is compatible with the theory of heterogeneous catalyst (L–H model). Thermodynamic and kinetic studies showed that photocatalytic reaction is endothermic and dye degradation follows the first-order kinetic model. The relative high value of activation energy confirms the effect of temperature to accelerate the photocatalytic degradation of DY86 in the presence of $TiO_2$. It was concluded that the kinetic of dye degradation also follows L–H model up to 120 mg/l and with further increase in dye concentration, rate constant values ($k_{obs.}$) are much less than that of calculated from L–H model.

# References

[1] N. Barka, S. Qourzal, A. Assabbane, A. Nounah, Y.A. Ichou, Photocatalytic degradation of an azo reactive dye, Reactive Yellow 84, in water using an industrial titanium dioxide coated media, Arab. J. Chem. 3 (2010) 279–283.

[2] G. Crini, Non-conventional low-cost adsorbents for dye removal: a review, Bioresour. Technol. 97 (2006) 1061–1085.

[3] M.A. Rauf, M.A. Meetani, S. Hisaindee, An overview on the photocatalytic degradation of azo dyes in the presence of TiO$_2$ doped with selective transition metals, Desalination 276 (2011) 13–27.

[4] S.K. Kansal, A.H. Ali, S. Kapoor, Photocatalytic decolorization of biebrich scarlet dye in aqueous phase using different nanophotocatalysts, Desalination 259 (2010) 147–155.

[5] M. Farbod, M. Khademalrasool, Synthesis of TiO$_2$ nanoparticles by a combined sol–gel ball milling method and investigation of nanoparticle size effect on their photocatalytic activities, Powder Technol. 214 (2011) 344–348.

[6] M.S. Sadjadi, N. Farhadyar, K. Zare, Synthesis of nanosize MCM-41 loaded with TiO$_2$ and study of its photocatalytic activity, Superlatt. Microstruct. 46 (2009) 266–271.

[7] P. Sathishkumar, R.V. Mangalaraja, S. Anandan, M. Ashokkumar, Photocatalytic degradation of ternary dye mixture in aqueous environment using gold nanoparticles loaded amino and mercapto functionalized TiMCM-41 nanocatalysts in the presence of visible light, Sep. Purif. Technol. 102 (2013) 67–74.

[8] H. Lachheb, O. Ahmed, A. Houas, J.P. Nogier, Photocatalytic activity of TiO$_2$–SBA-15 under UV and visible ligh, J. Photochem. Photobiol. A: Chem. 226 (2011) 1–8.

[9] W. Zhang, K. Wang, Y. Yu, H. He, TiO$_2$/HZSM-5 nano-composite photocatalyst: HCl treatment of NaZSM-5 promotes photocatalytic degradation of methyl orange, Chem. Eng. J. 163 (2010) 62–67.

[10] D.I. Petkowicz, S.B.C. Pergher, C.D.S. da Silva, Z.N. da Rocha, J.H.Z. dos Santos, Catalytic photodegradation of dyes by in situ zeolite-supported titania, Chem. Eng. J. 158 (2010) 505–512.

[11] A.N. Ejhieh, M. Khorsandi, Heterogeneous photodecolorization of Eriochrome Black T using Ni/P zeolite catalyst, Desalination 262 (2010) 79–85.

[12] F. Adam, J.N. Appaturi, Z. Khanam, R. Thankappan, M.A. Mohd Nawi, Utilization of tin and titanium incorporated rice husk silica nanocomposite as photocatalyst and adsorbent for the removal of methylene blue in aqueous medium, Appl. Surf. Sci. 264 (2013) 718–726.

[13] X. Huang, L. Li, X. Liao, B. Shi, Preparation of platinum nanoparticles supported on bayberry tannin grafted silica bead and its catalytic properties in hydrogenation, J. Mol. Catal. A: Chem. 320 (2010) 40–46.

[14] X. Huang, X. Liao, B. Shi, Tannin-immobilized mesoporous silica bead (BT–SiO$_2$) as an effective adsorbent of Cr(III) in aqueous solutions, J. Hazard. Mater. 173 (2010) 33–39.

[15] E. Binaeian, N. Seghatoleslami, M.J. Chaichi, Synthesis of oak gall tannin-immobilized hexagonal mesoporous silicate (OGT-HMS) as a new super adsorbent for the removal of anionic dye from aqueous solution, Desalin Water Treat. 57 (2016) 8420–8436.

[16] M. Labieniec, T. Gabryelak, Interactions of tannic acid and its derivatives (ellagic and gallic acid) with calf thymus DNA and bovine serum albumin using spectroscopic method, J. Photochem. Photobiol. B: Biol. 82 (2006) 72–78.

[17] P.T. Tanev, T.J. Pinnavaia, A neutral templating route to mesoporous molecular sieves, Science 267 (1995) 865–867.

[18] K.Y. Ho, G. McKay, K.L. Yeung, Selective adsorbents from ordered mesoporous silica, Langmuir 19 (2003) 3019–3024.

[19] X. Huang, Y. Wang, X. Liao, B. Shi, Adsorptive recovery of Au$^{3+}$ from aqueous solutions using bayberry tannin-immobilized mesoporous silica, J. Hazard. Mater. 183 (2010) 793–798.

[20] D.A. Skoog, D.M. West, F.J. Holler, S.R. Crouch, Fundamentals of Analytical Chemistry, eighth ed., Thomson Learning Academic Resource Center, 2004.

[21] T. Cetinkaya, L. Neuwirthova, K.R.M. Kutlakova, V.T. Sek, H. Akbulut, Synthesis of nanostructured TiO$_2$/SiO$_2$ as an effective photocatalyst for degradation of acid orange, Appl. Surf. Sci. 279 (2013) 384–390.

[22] J.S. Martin, M.G. Velasco, J.B. Heredia, J.G. Carvajal, J.S. Fernandez, Novel tannin-based adsorbent in removing cationic dye (Methylene Blue) from aqueous solution. Kinetics and equilibrium studies, J. Hazard. Mater. 174 (2010) 9–16.

[23] W. Baran, E. Adamek, A. Makowski, The influence of selected parameters on the photocatalytic degradation of azo-dyes in the presence of TiO$_2$ aqueous suspension, Chem. Eng. J. 145 (2008) 242–248.

[24] J. Saien, S. Khezrianjoo, Degradation of the fungicide carbendazim in aqueous solutions with UV/TiO$_2$ process: optimization, kinetics and toxicity studies, J. Hazard. Mater. 157 (2008) 269–276.

[25] E. Bizani, K. Fytianos, I. Poulios, V. Tsiridis, Photocatalytic decolorization and degradation of dye solutions and wastewaters in the presence of titanium dioxide, J. Hazard. Mater. 136 (2006) 85–94.

[26] J. Chen, L. Zhu, Heterogeneous UV-Fenton catalytic degradation of dyestuff in water with hydroxyl-Fe pillared bentonite, Catal. Today 126 (2007) 463–470.

[27] C.H. Wu, C.H. Yu, Effects of TiO$_2$ dosage, pH and temperature on decolorization of C.I. Reactive Red 2 in a UV/US/TiO$_2$ system, J. Hazard. Mater. 169 (2009) 1179–1183.

[28] H. Qi, L. Baoshun, Z. Zhengzhong, S. Mingxia, Z. Xiujian, Temperature effect on the photocatalytic degradation of Methyl Orange under UV–vis light irradiation, J. Wuhan Univ. Technol. -Mater. Sci. Ed. 25 (2010) 210–213.